Published in final edited form as:

Ann Surg. 2015 February ; 261(2): 395–404. doi:10.1097/SLA.0000000000000602.

Increased ^{18}F-FDG Uptake Is Predictive of Rupture in a Novel Rat Abdominal Aortic Aneurysm Rupture Model

Sean J. English, MD[*], **Morand R. Piert, MD**[†], **Jose A. Diaz, MD**[*], **David Gordon, MD**[‡], **Abhijit Ghosh, PhD**[*], **Louis G. D'Alecy, PhD**[§], **Steven E. Whitesall, BS**[§], **Ashish K. Sharma, MBBS**[¶], **Elise P. DeRoo, BA**[*], **Tessa Watt, BA**[*], **Gang Su, MD**[¶], **Peter K. Henke, MD**[*], **Jonathan L. Eliason, MD**[*], **Gorav Ailawadi, MD**[¶], and **Gilbert R. Upchurch Jr, MD**[¶]

[*]Section of Vascular Surgery, Conrad Jobst Vascular Research Laboratories, University of Michigan, Ann Arbor, MI

[†]Nuclear Medicine Division, University of Michigan, Ann Arbor, MI

[‡]Pathology Department, University of Michigan, Ann Arbor, MI

[§] Physiology Department, University of Michigan, Ann Arbor, MI

[¶]Vascular and Endovascular Surgery Division, University of Virginia, Charlottesville, VA.

Abstract

Objective—To determine whether ^{18}F-fluorodeoxyglucose (^{18}F-FDG) micro–positron emission tomography (micro-PET) can predict abdominal aortic aneurysm (AAA) rupture.

Background—An infrarenal AAA model is needed to study inflammatory mechanisms that drive rupture. ^{18}F-FDG PET can detect vascular inflammation in animal models and patients.

Methods—After exposing Sprague-Dawley rats to intra-aortic porcine pancreatic elastase (PPE) (12 U/mL), AAA rupture was induced by daily, subcutaneous, β-aminopropionitrile (BAPN, 300 mg/kg, N = 24) administration. Negative control AAA animals (N = 15) underwent daily saline subcutaneous injection after PPE exposure. BAPN-exposed animals that did not rupture served as positive controls [nonruptured AAA (NRAAA) 14d, N = 9]. Rupture was witnessed using radiotelemetry. Maximum standard uptakes for ^{18}F-FDG micro-PET studies were determined. Aortic wall PAI-1, uPA, and tPA concentrations were determined by western blot analyses. Interleukin (IL)-1β, IL-6, IL-10, and MIP-2 were determined by Bio-Plex bead array. Neutrophil and macrophage populations per high-power field were quantified. Matrix metalloproteinase (MMP) activities were determined by zymography.

Results—When comparing ruptured AAA (RAAA) to NRAAA 14d animals, increased focal ^{18}F-FDG uptakes were detected at subsequent sites of rupture (P = 0.03). PAI-1 expression was significantly less in RAAA tissue (P = 0.01), with comparable uPA and decreased tPA levels (P = 0.02). IL-1β (P = 0.04), IL-6 (P = 0.001), IL-10 (P = 0.04), and MIP-2 (P = 0.02)expression,

Reprints: Gilbert R. Upchurch, Jr, MD, University of Virginia, PO Box 800679, Charlottesville, VA 22908. gru6n@virginia.edu..

Disclosure: The authors declare no conflicts of interest.

Supplemental digital content is available for this article. Direct URL citations appear in the printed text and are provided in the HTML and PDF versions of this article on the journal's Web site (www.annalsofsurgery.com).

neutrophil ($P = 0.02$) and macrophage presence ($P = 0.002$), and MMP9 ($P < 0.0001$) activity were increased in RAAA tissue.

Conclusions—With this AAA rupture model, increased prerupture ^{18}F-FDG uptake on micro-PET imaging was associated with increased inflammation in the ruptured AAA wall. ^{18}F-FDG PET imaging may be used to monitor inflammatory changes before AAA rupture.

Keywords

AAA rupture; FDG-PET; IL-6; macrophage; MMP

Abdominal aortic aneurysm (AAA) is a significant medical problem, with a high mortality rate. More than 50% of AAA patients present with rupture, without a previous AAA diagnosis. Currently, increased aortic diameter represents the greatest risk measurement for human AAA rupture; however, small AAAs rupture, whereas large AAAs are incidentally discovered. Clinical practice would benefit from a reliable, noninvasive test of impending aortic rupture.

Inflammation, specifically infiltration by activated macrophages, plays a significant role in AAA development and rupture. Glucose is the primary energy source for inflammatory cells, including macrophages. A number of studies have suggested a role for ^{18}F-fluorodeoxyglucose (^{18}F-FDG) positron emission tomography (PET) imaging to detect aortic wall inflammation.[1] Sakalihasan et al[2] correlated increased AAA ^{18}F-FDG uptake with associated symptoms and rapid aortic enlargement.

The process of aortic rupture remains poorly understood, with a lack of adequate noninvasive imaging and biological insight. We utilized the lysyl oxidase inhibitor β-aminopropionitrile (BAPN) with the porcine pancreatic elastase (PPE) model to generate a novel, reproducible model of AAA rupture in the rat. We hypothesized that aortic rupture would be associated with an increased inflammatory response in the AAA wall, and this increased inflammation could be identified noninvasively by ^{18}F-FDG micro-PET.

METHODS

Male Sprague-Dawley rats (200–300 g) were obtained from Charles River Laboratories (Wilmington, MA) and utilized for all experiments. All surgical procedures were approved by the University of Michigan Universal Committee on the Use and Care of Animals (Protocol 10430).

Ruptured AAA Model

Starting 3 days before PPE exposure, the negative control AAA (CAAA) (N = 15) group underwent normal saline administration (3 mL/kg subcutaneously daily), and another group of AAA animals (N = 24) underwent BAPN administration (300 mg/kg, 100 mg/mL, 3 mL/kg subcutaneously daily), referred to as the BAPN group (Fig. 1). PPE (12 U/mL) was instilled into the isolated aortic segment for 30 minutes. During PPE infusion, average increases in aortic diameter of 58.6 ± 2.8% and 52.8 ± 2.7% [mean ± standard error of the mean, P = not significant (NS)] were generated for the CAAA and BAPN groups,

respectively. Upon reestablishment of segmental blood flow, the CAAA and BAPN groups demonstrated aortic diameter increases of 54.9 ± 2.7% and 48.5 ± 2.2% (*P* = NS), respectively. The CAAA group received normal saline subcutaneously daily until harvested on day 6 post-PPE exposure (CAAA 6d, N = 7) or day 14 post-PPE exposure (CAAA 14d, N = 8). The BAPN group received BAPN subcutaneously daily until rupture or harvest on day 14 post-PPE exposure. All animals that ruptured over the course of the study were included in the ruptured AAA (RAAA) group (N = 15), whereas those animals that did not rupture by day 14 post PPE were referred to as the nonruptured AAA group [ruptured AAA (NRAAA) 14d, N = 9] (Supplemental Digital Content Figure 1, available at http://links.lww.com/SLA/A540). Postoperative analgesia was not used during this study.[3]

Blood Pressure Telemetry

After establishing the PPE model, CAAA (N = 3) and BAPN (N = 9) exposed rats were instrumented with radiotelemetric monitoring devices (PA-C10; Data Science, St Paul, MN) during the same anesthetic exposure. Ultimately, NRAAA 14d (N = 4) and RAAA (N = 5) were evaluated with telemetric monitoring. PA-C10 devices provided continuous, unrestrained blood pressure (BP) and heart rate monitoring, considering 1 hour moving averages. Data acquisition and management were previously described.[4] A custom Microsoft Excel (Microsoft, Redmond, WA) macro was utilized to alert the author by telephone that a sustained systolic BP threshold of less than 50 mm Hg had been passed, representing AAA rupture.

Noninvasive Aortic Diameter Measurements Using Ultrasound

Aortic diameters were measured with ultrasound (12 MHz Zonare, Mountain View, CA) as described by Knipp et al.[5] Percent increases in aortic diameter were determined considering the average baseline intraluminal aortic diameter and the maximum aortic diameter 3, 6, and 14 days post-PPE exposure.

^{18}F-FDG Micro-PET

Six days after PPE exposure, CAAA 6d (N = 5) and BAPN (N = 14) animals underwent dynamic ^{18}F-FDG PET for approximately 90 minutes, on a micro-PET R4 scanner (Concorde/Siemens Microsystems, Knoxville, TN).[6] Retrospectively, considering the BAPN group, 2 groups were considered: those animals that received BAPN but did not rupture, NRAAA 6d (N = 3), and those that did rupture, RAAA 6d (N = 10). Fourteen days after PPE exposure, CAAA 14d (N = 8) underwent the same imaging protocol.[7] AAAs were identified on early bolus images, whereas late phase ^{18}F-FDG uptake (between 60 and 90 minutes) was used for further data analysis. Considering focal areas of maximal, left anterolateral AAA ^{18}F-FDG uptake, maximum standard uptake values (SUV_{max}) were determined for control AAAs and BAPN-exposed AAAs that ultimately ruptured.[8]

Histology and Immunohistochemistry

Modified from Diaz et al[9] trichrome stained sections were analyzed, and aortic wall fibrotic area percentages were determined. Immunohistochemical staining of rat neutrophils and macrophages were performed using antirat neutrophil (1:325, Accurate Chem, Westbury,

NY) and antirat CD68[10] (1:250, Accurate Chem, Westbury, NY) primary antibodies, respectively. Utilizing a Leica DMR microscope (Leica Microsystems IN, Buffalo Grove, IL), motorized stage, Stereo Investigator software (Version 4.34; Microbrightfield Inc, Williston, VT), mural thrombus and total AAA wall areas (μm^2), as well as CD68 positive cell counts per high power field (HPF) were determined (mean 133 HPFs at 63×). A blinded, board-certified cardiovascular pathologist validated the histological and immunohistochemical assessments.

Cytokine Assessment and Western Blot Analysis

Cytokine content in rat aortic tissue homogenates was quantified using the Bio-Plex bead array technique using a multiplex cytokine panel assay (Bio-Rad Laboratories, Hercules, CA). Tissue inhibitor of metalloproteinase 1 (TIMP-1) concentrations were determined in terms of mean pixel intensity using a Proteome Profiler Array Rat Cytokine Array Panel A (R&D Systems, Inc, Minneapolis, MN), and array data were developed on x-ray film and quantified using Image Lab software (Version 3.0; Bio-Rad Laboratories, Hercules, CA). Western blot analyses for uPA, tPA, and PAI-1 protein concentrations were performed in a standard fashion.

Matrix Metalloproteinase (MMP) Activity by Zymography

Protein isolation, from ruptured AAA tissue and control aortic tissue at 6 days post-PPE exposure, was performed in a standard fashion. Total MMP9 and active MMP2 activities, in terms of integrated optical density (IOD), were observed by clear bands against a blue background.[11]

Data Analysis

Statistical analyses were performed using Prism 5 (GraphPad Software, Inc, La Jolla, CA). Quantitative results were analyzed by unpaired 2-tailed Student *t* tests, with a Welch's correction, and *P* values less than 0.05 were considered statistically significant. Linear regression was performed, and a coefficient of determination was reported. A Kaplan-Meier curve was generated to assess the survival of BAPN-exposed animals. Data are presented as mean ± standard error of the mean.

RESULTS

Aortic Diameter Increases and Rupture Rate

Comparable mean 3-day aortic diameter increases of 98.0 ± 7.7%, 99.1 ± 6.7%, and 107.2 ± 6.1% were observed for the CAAA (N = 11), NRAAA (N = 9), and RAAA (N = 14) groups, respectively. Comparable mean 6-day aortic diameter increases of 258.3 ± 30.9%, 221.4 ± 16.2%, and 276.2 ± 30.2% were observed for the CAAA (N = 12), NRAAA (N = 8), and RAAA (N = 12) groups, respectively. At 14 days post-PPE exposure, mean aortic diameters remained comparable for CAAA and NRAAA groups at 554.6 ± 63.3% and 540.9 ± 48.9% (*P* NS), respectively. No statistically significant differences in mean aortic diameter increases were noted between the groups at each time point (Supplemental Digital Content Figure 2, available at http://links.lww.com/SLA/A540).

Rupture occurred in 63% of BAPN-exposed animals. AAA ruptures occurred 6 to 10 days after PPE exposure. A Kaplan-Meier Curve demonstrates survival associated with BAPN administration (Supplemental Digital Content Figure 3, available at http://links.lww.com/SLA/A540). Left retroperitoneal hemorrhage and the rupture site were identified in every case at AAA harvest (Supplemental Digital Content Figure 4, available at http://links.lww.com/SLA/A540). In each case, rupture occurred along the left, anterolateral AAA wall, as determined at the time of autopsy. No rupture occurred in negative control animals.

No Changes in Heart Rate or BP Associated With BAPN Administration as Measured by Telemetry

Telemetry was considered for CAAA (N = 3), NRAAA (N = 4), and RAAA (N = 5). Mean heart rates (HRs) of 370 ± 16 and 317 ± 5 were determined for the CAAA and NRAAA groups 6 days after PPE exposure, respectively. A mean HR of 365 ± 20 was determined for the RAAA group 24 hours before rupture, and the average HR over 1-hour preceding rupture was 371 ± 19. No significant differences in HR were identified comparing the 3 groups 6 days after PPE exposure or 24 hours before rupture. Mean systolic/diastolic/mean BPs for CAAA, NRAAA, and RAAA were determined. Mean BPs of 123/99/114 mm Hg and 114/87/102 mm Hg were determined for CAAA and NRAAA animals 6 days after PPE exposure, respectively. A mean BP of 119/88/105 mm Hg was determined for RAAA rats 24 hours before rupture. The average BP over 1-hour preceding rupture was 130/99/116 mm Hg, and no significant differences in BP were identified comparing the 3 groups 6 days after PPE exposure or 24 hours before rupture. All animals that underwent continuous telemetric monitoring demonstrated stable HRs and BPs throughout the observation period that fell within an accepted normal range for rats. Utilizing the alarm triggered by a significant decrease in BP, all RAAA tissues were harvested within 1.5 hours of rupture (Supplemental Digital Content Figure 5, available at http://links.lww.com/SLA/A540).

Increased Focal ^{18}F-FDG Uptake in AAA Walls That Ultimately Ruptured

Areas of increased focal ^{18}F-FDG uptake were noted in the rupture group along the left anterolateral AAA wall and correlated with subsequent sites of AAA rupture (Fig. 1). The distance from the iliac bifurcation to the approximate midpoint of the rupture site was measured by video micrometry at 0.75× magnification, and comparable distances on micro-PET imaging were measured from the iliac bifurcation to the region of highest ^{18}F-FDG uptake (N = 6). Mean distances of 12.4 ± 0.7 mm and 12.1 ± 0.6 mm were determined considering sites of rupture and greatest focal ^{18}F-FDG uptake, respectively, and linear regression was performed using these distances (R^2 = 0.94, P = 0.001). Considering regions of greatest left anterolateral ^{18}F-FDG uptake, SUV_{max} values of 1.4 ± 0.1, 0.9 ± 0.1, 1.4 ± 0.3, and 2.5 ± 0.3 were determined for the CAAA 6d (N = 5), CAAA 14d (N = 8), NRAAA 6d (N = 3), and RAAA 6d (N = 7) groups, respectively, and RAAA animals demonstrated significantly greater ^{18}F-FDG uptake than the negative and positive controls (Fig. 1).

Mural Thrombus Is Associated With the PPE AAA Model and Decreased Collagen Content, as Well as Increased Neutrophil and Macrophage Presence in RAAA Tissue

No evidence of aortic dissection was noted in any control or ruptured case. Similar to human AAAs, mural thrombus was observed in nearly every control and ruptured case, as determined by a cardiovascular pathologist (D.G.). Comparable mural thrombus area (μm^2) to total AAA wall area (μm^2) ratios of 0.22 ± 0.03, 0.35 ± 0.06, 0.31 ± 0.04, and 0.30 ± 0.06 were determined for the CAAA 6d (N = 6), CAAA 14d (N = 6), NRAAA 14d (N = 6), and RAAA (N = 5) groups, respectively. Aortic wall fibrotic area percentages of 10.4 ± 2.5%, 25.9 ± 2.3%, 20.8 ± 1.4%, and 11.1 ± 1.6% were determined for CAAA 6d (N = 7), CAAA 14d (N = 6), NRAAA 14d (N = 8), and RAAA (N = 6) tissue, respectively (Supplemental Digital Content Figure 6, available at http://links.lww.com/SLA/A540). Neutrophil populations of 1.4 ± 0.2, 0.5 ± 0.1, 0.3 ± 0.1, and 1.1 ± 0.2 positive neutrophils per high power field were observed for the CAAA 6d (N = 7), CAAA 14d (N = 8), NRAAA 14d (N = 9), and RAAA (N = 7)groups, respectively. Macrophage populations of 0.6 ± 0.1, 0.3 ± 0.1, 0.09 ± 0.02, and 1.0 ± 0.1 CD68-positive macrophages per high power field were observed for the CAAA 6d (N = 6), CAAA 14d (N = 6), NRAAA 14d (N = 6), and RAAA (N = 7) groups, respectively. Qualitatively, increased macrophages were noted at the wall-mural thrombus interface, and increased neutrophils were noted in the mural thrombus. RAAA tissue demonstrated significantly increased numbers of neutrophils and macrophages compared with nonruptured positive control tissue (Fig. 2).

Increased Fibrinolytic Activity in the RAAA Wall

Serine protease activity in the RAAA wall was variable compared to negative and positive control tissue. Normalized intensities relative to Ponceau stain for uPA were 6.4 ± 0.4, 3.9 ± 0.5, 7.5 ± 0.4, and 7.3 ± 0.4 for CAAA 6d, CAAA 14d, NRAAA 14d, and RAAA, respectively. Normalized intensities relative to Ponceau stain for tPA were 0.6 ± 0.2, 3.1 ± 0.5, 4.3 ± 0.7, and 2.0 ± 0.2 for CAAA 6d, CAAA 14d, NRAAA 14d, and RAAA, respectively. Normalized intensities relative to Ponceau stain for active PAI-1 were 2.6 ± 0.4, 2.2 ± 0.5, 1.3 ± 0.3, and 0.3 ± 0.1 for CAAA 6d, CAAA 14d, NRAAA 14d, and RAAA, respectively. Less tPA secretion in the RAAA wall was observed compared to NRAAA 14d tissue ($P = 0.02$) and comparable levels of uPA in the walls of NRAAA 14d and RAAA tissue (P = NS). No significant difference in active PAI-1 expression was observed when comparing CAAA 14d and NRAAA 14d tissue (P = NS). However, there was significantly less active PAI-1 expression in RAAA tissue compared with CAAA 14d ($P = 0.006$) and NRAAA 14d tissue ($P = 0.01$) (Fig. 3).

Increased IL-1β, IL-6, IL-10, MIP-2 Expression in Ruptured AAA tissue

IL-6 expression by RAAA tissue was significantly greater than either negative control group or the positive control group, and IL-1β, IL-10, and MIP-2 expression by RAAA tissue was significantly greater than NRAAA 14d tissue in each case (Supplemental Digital Content Figure 7, available at http://links.lww.com/SLA/A540). Utilizing a Bio-Plex bead array, IL-1β concentrations of 799 ± 156 pg/mL, 544 ± 123 pg/mL, 405 ± 102 pg/mL, and 1767 ± 548 pg/mL were determined for CAAA 6d (N = 6), CAAA 14d (N = 8), NRAAA 14d (N = 8), and RAAA (N = 8) tissue, respectively. We observed significantly greater IL-1β

expression in RAAA tissue than in NRAAA tissue ($P = 0.04$). IL-6 concentrations of 317 ± 31 pg/mL, 166 ± 21 pg/mL, 108 ± 12 pg/mL, and 2500 ± 457 pg/mL were determined for CAAA 6d (N = 5), CAAA 14d (N = 7), NRAAA 14d (N = 8), and RAAA (N = 8) tissue, respectively. We observed significantly greater expression by RAAA tissue than by CAAA 6d ($P = 0.002$), CAAA 14d ($P = 0.001$), and NRAAA 14d (0.001) tissues. IL-10 concentrations of 320 ± 23 pg/mL, 222 ± 10 pg/mL, 157 ± 23 pg/mL, and 288 ± 50 pg/mL were determined for CAAA 6d (N = 6), CAAA 14d (N = 8), NRAAA 14d (N = 8), and RAAA (N = 8) tissues, respectively. In particular, we observed significantly greater IL-10 expression by RAAA tissue than by NRAAA 14d tissue ($P = 0.04$). MIP-2 concentrations of 16 ± 2 pg/mL, 7 ± 1 pg/mL, 5 ± 1 pg/mL, and 12 ± 2 pg/mL were determined for CAAA 6d (N = 6), CAAA 14d (N = 7), NRAAA 14d (N = 7), and RAAA (N = 7) tissues, respectively (Supplemental Digital Content Figure 7, available at http://links.lww.com/SLA/A540).

Increased MMP9 Activity in Ruptured AAAs

MMP activity in ruptured AAA tissue was greater than that in negative and positive control AAA tissue. IODs for total MMP9 of $1.3 \pm 0.5 \times 10^5$, $2.1 \pm 0.3 \times 10^5$, $1.4 \pm 0.2 \times 10^5$, and $3.3 \pm 1.8 \times 10^5$ were determined for CAAA 6d (N = 4), CAAA 14d (N = 6), NRAAA 14d (N = 6), and RAAA (N = 6) tissue, respectively. IODs for active MMP2 of $1.8 \pm 0.9 \times 10^4$, $5.4 \pm 0.8 \times 10^4$, $7.9 \pm 1.3 \times 10^4$, and $7.4 \pm 1.9 \times 10^4$ were determined for CAAA 6d (N = 4), CAAA 14d (N = 6), NRAAA 14d (N = 5), and RAAA (N = 6) tissue, respectively (Supplemental Digital Content Figure 8, available 4), at http://links.lww.com/SLA/A540).

DISCUSSION

In this study, we have developed a reliable model of infrarenal AAA rupture in the rat. We have demonstrated that BAPN does not cause hemodynamic effects over the course of administration or at the time of AAA rupture. For the first time, ^{18}F-FDG micro-PET was utilized to noninvasively identify the location of subsequent rat AAA rupture. In addition, uPA levels were globally increased in the AAA tissue, with similar levels when comparing positive control AAA tissue and ruptured AAA tissue, with significantly lower levels of active PAI-1 when comparing ruptured AAA tissue to positive control AAA tissue. Furthermore, we documented increased IL-1β, IL-6, IL-10, MIP-2 expression, neutrophil and macrophage infiltration, and total MMP9 activity in the ruptured AAA wall compared with positive control AAA wall tissue.

Regarding human data to date, there is mixed data regarding the ability of ^{18}F-FDG PET to detect inflammation associated with human AAA growth and subsequent rupture. Kotze et al[12] demonstrated an inverse relationship between ^{18}F-FDG uptake and AAA expansion, when considering AAA patients (N = 25). However, Truijers et al[13] demonstrated greater ^{18}F-FDG uptake in AAAs (N = 34), in terms of SUV_{max}, compared with nonaneurysmal aortas.[13] Furthermore, Sakalihasan et al[2] evaluated 10 AAA patients with positive ^{18}F-FDG uptake in the AAAs, and 5 of these patients required urgent AAA repair within 2 to 30 days of their scans due to rapid expansion and/or rupture. In a follow-up manuscript, Sakalihasan et al[14] identified 9 of 10 patients with positive AAA ^{18}F-FDG uptake that required repair for AAA rupture (N = 1), rapid expansion (N = 2), or pain

associated with their AAA (N = 5). Considering 3 symptomatic AAA patients, Reeps et al[15] demonstrated significantly increased ^{18}F-FDG AAA uptake that correlated with greater macrophage populations on AAA wall histology, as well as higher MMP9 expression and decreased collagen fiber content, when tissue was taken at the time of repair. In a follow-up manuscript, Reeps et al demonstrated the ability to discriminate between symptomatic (N = 5) and asymptomatic (N = 18) AAA patients on the basis of ^{18}F-FDG uptake. They then correlated this increased ^{18}F-FDG uptake with aortic wall macrophage infiltration and MMP9 expression.[16] We believe that there is sufficient human data to warrant further study of our rat AAA rupture model and the ability of ^{18}F-FDG mirco-PET to predict rupture associated with this model, as well as to prospectively study the ability of ^{18}F-FDG PET, perhaps using other radiotracers capable of identifying sites of increased inflammation, in an effort to predict human AAA rupture.

Thus far, few studies have evaluated the use of ^{18}F-FDG PET to assess inflammation associated with a rodent model of AAA development. Sarda-Mantel et al[17] correlated significantly greater ^{18}F-FDG uptake with the presence of macrophages for AAAs generated utilizing the orthotopic implantation of decellularized guinea pig abdominal aorta in Lewis rats. To further assess the inflammation of a more dynamic process, Patel et al[18] demonstrated significantly greater inflammation and ^{18}F-FDG uptake by atherosclerotic rabbit aortas treated to trigger plaque rupture. We observed significantly less focal uptake of ^{18}F-FDG along the left anterolateral AAA wall of CAAA 14d compared with CAAA 6d animals, and this is consistent with the decreased presence of neutrophils and macrophages noted on IHC and the correlated decreased cytokine milieu. We observed no significant differences in focal uptake when comparing the negative control animals to the positive control group; however, we were only able to consider 3 NRAAA 6d animals, and additional positive control animals will be considered in the future. A group of positive control animals were not imaged at 14 days post-PPE exposure. Four (27%) RAAA animals ruptured 10 days post-PPE exposure, and this would have been a reasonable group to consider; however, given that the negative control group demonstrated decreased ^{18}F-FDG uptake at 14 days, the positive control group would have likely demonstrated similarly decreased uptake at 14 days. Greater diffuse ^{18}F-FDG up-take was noted in the walls of the NRAAA 6d animals; however, significantly greater focal uptake was noted in rats that went on rupture postimaging. This is consistent with the previously described work performed with patients.[15,16] It should be noted that the sutured aortotomy site was identified in each rupture case, and this location was distal and medial to the site of rupture in every case.

To date, our understanding of the biology associated with ruptured AAA is lacking. In this study, anatomic and physiologic similarities and differences between our model of AAA rupture and human disease were defined. In the classic manuscript by Darling, 31 ruptures were observed on the left side of the aorta, whereas 24 ruptures were observed on the right side of the aorta. Furthermore, 86% of ruptures that they described occurred in the retroperitoneum.[19] This is consistent with more recent wok by Assar and Zarins[20] describing retroperitoneal rupture in 80% of human cases. We observed rupture in a left anterolateral location into the retroperitoneum in all cases of the model. Given the retroperitoneal dissection that was performed for PPE exposure, it must be noted that the retroperitoneum was compromised, and the retroperitoneal location for rupture may be dictated in part by the

retroperitoneal scar tissue that forms after PPE exposure. A significant association between hypertension and human-ruptured AAA presentation has been observed; in particular, early morning peaks in BP associated with the diurnal variations have been associated with the time of symptom onset, time of presentation, and ultimate human AAA rupture.[21] Kanematsu et al[22] described no changes in BP associated with subcutaneous administration of BAPN (150 mg/kg) to C57BL/6J mice, and in our study, BAPN administration did not cause increases in BP over the course of exposure on telemetry when compared with negative and positive control animals. Furthermore, AAA rupture occurred without terminal increases in BP events. The number of negative control animals should be increased with future work to address the possibility of statistical significance, but this suggests that increased BP is likely not associated with this model AAA rupture and does not mimic human disease in this regard.

With the exception of the Apo E −/− mouse that undergoes angiotensin II infusion, which generates primarily suprarenal aortic aneurysms, associated with dissections, that rupture in 20% to 30% of cases, there is no reliable model of infrarenal AAA rupture.[23] Compared with previous work, BAPN did not cause aortic dissection in a single control or ruptured AAA in this study.[24] Our use of BAPN with the PPE model does not generate AAAs with evidence of atherosclerosis; however, the medial degeneration[25] that we have observed in the setting of BAPN administration has been observed in human aneurysms that develop secondary to aging and atherosclerosis. Furthermore, mural thrombus was noted in nearly every control and ruptured case in our study. Mural thrombus is representative of human disease and is believed to play an integral role in the processes of AAA dilation and ultimate rupture, due in part to the hypoxic environment created by mural thrombus.[26] Comparable intraluminal thrombus (ILT) volume to AAA volume ratios have been observed with intact and ruptured AAAs in humans,[27] and we observed no significant differences in mural thrombus area to total AAA wall area ratios when comparing the negative and positive controls, as well as ruptured AAA samples.

It has been proposed that plasmin is a potent activator of pro-MMPs, and the fibrinolytic system components are synthesized, stored, and released from the mural thrombus and AAA wall.[28] It is believed that endothelial cells predominantly release tPA, neutrophils store and release uPA from granules,[29] and platelets store and secrete PAI-1 from alpha granules,[30] whereas PAI-1 is also produced by the endothelium.[31] Platelets have been shown to recruit neutrophils at the thrombus surface via the interaction of platelet exposed P selectin with neutrophil PSGL-1.[32] The initial increase in neutrophils seen in CAAA 6d tissue seems to be associated with the subacute phase of the PPE model and the presence of mural thrombus. A significant decrease was observed in the neutrophil population from 6 to 14 days ($P = 0.003$), and this is consistent with a transition from the subacute phase to the chronic phase of the PPE AAA model. Comparable number of neutrophils in the CAAA 14d and NRAAA 14d tissues, with increased neutrophil populations in RAAA tissue, suggests that neutrophils continue to play a role in the AAA development and subsequent rupture, independent of BAPN administration. Although we did not specifically quantify neutrophil populations in the thrombus itself, qualitatively, neutrophils appeared to represent the predominate cell type in the ILT. Neutrophils are the first cell type to infiltrate a thrombus,[33]

and MIP-2 plays a chemotactic role for neutrophils during an inflammatory process.[34] In this study, greater neutrophil infiltration in ruptured AAA tissue is further supported by an increase in MIP-2 expression by RAAA tissue compared with NRAAA 14d tissue (P = 0.02). However, it would seem that BAPN stimulation, with ILT and neutrophil infiltration, causes an additional increase in uPA secretion given the significantly greater degree of uPA expression identified in NRAAA 14d tissue compared with CAAA 14d tissue (P = 0.0001). It has been demonstrated that endothelium denudation occurs with implementation of the PPE AAA model,[35] and it has been demonstrated that BAPN causes increased formation of internal elastic lamina ruptures in Brown Norway normotensive rats.[36] BAPN administration in the setting of the PPE model results in further decreased tPA and PAI-1 expression in those AAAs that ultimately rupture, and this may be due to sustained effects on the endothelium and/or AAA wall over the course of BAPN administration.

The role of inflammatory mediators in the processes of AAA growth and rupture is poorly understood. We have demonstrated that IL-1β is critical for AAA initiation and progression associated with the PPE AAA model in rodents.[37] IL-1β is an early inflammatory marker and leads the inflammatory cascade resulting in the stimulation of IL-6 secretion and macrophage infiltration,[38] and we observed significantly greater IL-1β expression in RAAA tissue compared with nonruptured AAA tissue. Aortic explant cultures from human-ruptured AAAs have demonstrated increased secretory levels of proinflammatory cytokines, including IL-6, compared with that of nonruptured AAAs. Secretory levels of IL-6 were not correlated with the size of ruptured AAAs, suggesting a role for IL-6 in the rupture process independent of size and the process of expansion.[39] Furthermore, others have described significantly greater plasma concentrations of IL-6 in ruptured AAA patients compared with AAA patients operated on electively.[40] It has been demonstrated that increased IL-6 expression results in an upregulation of CCL2 leading to monocyte recruitment in a mouse model of deep vein thrombosis.[41] We observed significantly greater IL-6 expression by RAAA tissue compared with CAAA 6d (P = 0.002), CAAA 14d (P = 0.001), and NRAAA 14d (0.001) tissues suggesting a possible role for IL-6 in the AAA rupture process. Wallinder et al[42] described significantly elevated circulating levels of IL-10, an anti-inflammatory cytokine, in patients operated on for ruptured AAA compared with nonruptured AAA, in the setting of significantly increased circulating levels of IL-6. As a possible correlate of anti-inflammatory activity, we considered IL-10 expression, and we observed significantly greater IL-10 expression by RAAA tissue compared with NRAAA 14d tissue. IL-10 expression by CAAA 6d tissue that was comparable with RAAA tissue suggests that the level of expression is associated with the subacute phase of the PPE AAA model. The significant decrease that occurs in CAAA 14d compared with CAAA 6d likely represents a transition from the subacute phase to the chronic phase of the PPE AAA model. Given that IL-10 is known to negatively regulate IL-6 production, it is possible that significantly lower total levels of IL-10 compared with IL-6 levels are observed in RAAA tissue given the significant upregulation and expression of IL-6.

The assessment of human-ruptured AAA tissue to date has been limited. A secondary role of the fibrinolytic system is tissue remodeling, and uPA is believed to play an integral role in this process. This remodeling process specifically involves MMPs in the presence of

recruited macrophages, and uPA regulates gene expression and synthesis of MMP9 and induces secretion of MCP-1 for monocyte recruitment.[43] Furthermore, in a mouse model of inflammation, macrophage recruitment was significantly increased in PAI-1 −/− mice.[44] Morphometric analysis of human tissue has demonstrated significantly greater macrophage populations in ruptured AAA tissue compared with intact AAA tissue.[45] We observed significantly increased macrophage populations in RAAA tissue compared with NRAAA 14d tissue, and this is consistent with a cytokine profile representative, in part, of increased macrophage presence and/or activity. Our observation of decreased macrophage populations in CAAA 14d tissue compared with CAAA 6d tissue is consistent with our earlier work evaluating macrophage infiltration in the PPE-exposed mouse aorta at 7 and 14 days post-PPE exposure.[46] Furthermore, this is consistent with the decreased expression of IL-6 by CAAA 14d tissue compared with that of CAAA 6d tissue. It is interesting to see significantly lower macrophage populations in NRAAA 14d tissue compared with either CAAA group, specifically the CAAA 14d group, but again, this is consistent with the significantly lower levels of IL-6 and IL-10 expression. This suggests that a decrease in macrophage infiltration into the BAPN-stimulated PPE AAA wall may be associated with a decreased risk of rupture. The lack of a statistically significant difference in macrophage presence in RAAA tissue compared with that of CAAA 6d tissue suggests that the infiltration of macrophages is in part due to the subacute phase of the PPE AAA model.

Increased MMP2 and MMP9 activities have been observed in human-ruptured AAA tissue, and it is believed that MMP2 contributes to AAA expansion, whereas MMP9 contributes to ultimate rupture.[47] Hurks et al described significantly greater MMP2 and MMP9 activities in the lateral walls of human AAAs than in the dorsal and ventral walls.[48] With ruptured rat AAA tissues that were all harvested within 1.5 hours of AA rupture, we observed comparable MMP2 levels in NRAAA 14d and RAAA tissues for AAAs of comparable size before AAA rupture. We also observed significantly increased MMP9 activity in RAAA tissue compared with positive control AAA tissue. It must be noted that Kurihara et al[49] have demonstrated aortic intimal infiltration by neutrophils that release MMP9 in the setting of BAPN administration to wild-type mice that also received angiotensin II and develop acute aortic dissection. With both neutrophil and macrophage populations increased in RAAA tissue, it is possible that both cell types secrete MMP9 that contributes to the ultimate rupture process. TIMP-1 is a specific endogenous inhibitor of MMP9, and the expression of both proteins has been correlated with pathologic processes involving the degradation and accumulation of the extracellular matrix.[50] Khan et al[51] demonstrated a positive correlation between ILT thickness and concentrations of TIMP-1 and active MMP9 in AAA tissue compared with control aortic tissue. Compared with CAAA 14d and NRAAA 14d tissues, we observed significantly greater TIMP-1 protein levels in RAAA tissue by protein array analysis (Supplemental Digital Content Figure 9, available at http://links.lww.com/SLA/A540). This suggests that increased TIMP-1 expression may serve as a compensatory response to the significant increase in MMP9 expression and activity.

In an effort to address whether it is an inflammatory response that leads to the process of rupture or whether it is an inflammatory response that occurs acutely at the time of rupture, we considered a group of PPE-exposed AAA animals that received BAPN but were harvested before rupture could occur (BAPN 6d); this group of animals could also be

considered a positive 6-day control group (NRAAA 6d). When assessing neutrophil populations, we observed populations in BAPN 6d tissue that were comparable with those of CAAA 6d (P = 0.99) and RAAA (P = 0.50) tissues; however, BAPN 6d neutrophil populations were less than CAAA 14d tissues (P = 0.05) and greater than NRAAA 14d tissues (P = 0.05). We speculate that neutrophils seem to play a role in the development of rupture associated with this model, likely in response to the presence of mural thrombus; however, the presence of neutrophils in the BAPN 6d tissue is certainly consistent with the subacute phase of the PPE AAA model.[52] Regarding macrophage presence, we observed significantly fewer macrophages in the NRAAA 14d group than in the CAAA 14d group; therefore, there seems to be an effect of BAPN administration on the NRAAA 14d group that is independent of a time-dependent decrease in inflammation. We observed a greater number of macrophages in BAPN 6d AAA tissue compared with NRAAA 14d tissue that did not reach statistical significance. This may be due to the small number of BAPN 6d animals considered (N = 4). It is interesting to observe that one animal demonstrated 0.97 CD68-positive macrophages per HPF, whereas the remaining 3 animals demonstrated a mean of 0.20 ± 0.05 CD68-positive macrophages per HPF. The mean CD68-positive macrophage count per HPF for RAAA tissue was 0.85 ± 0.14, whereas the mean value for NRAAA 14d tissue was 0.09 ± 0.02. It is plausible that one rat may have gone on to rupture, whereas the remaining 3 rats may not have ruptured over the allowed 14-day period. Given the role that MMP9 is believed to play in the ultimate process of rupture, it should also be noted that no differences in total MMP9 activity were observed between the negative and positive control groups at 6 and 14 days, but there was significantly greater MMP9 activity found in RAAA tissue.[53] It is unlikely that there is a difference when considering BAPN 6d tissue. The BAPN 6d group is one that is made up of 2 groups: one that will go on to rupture and the other that will not. Therefore, comparisons with the other experimental groups are not clear given that a mean numerical assessment of the BAPN 6d group will be skewed by the predominance of either animals that will go on to rupture or those that will not. Considering a larger number of the animals for this group will hopefully allow us to identify the 2 groups and predict as to which animals will go on to rupture, and this is something that we will explore in the future. The ability to possibly predict AAA rupture as a function of inflammatory cell infiltration and activity supports the need for a sensitive noninvasive method that can detect this metabolic activity and aid in determining AAA rupture risk in patients.

Collagen degradation is thought to play an integral role in AAA rupture.[54] Reeps et al[15] demonstrated that collagen content negatively correlated with FDG uptake and MMP9 presence in human AAA tissue. Huffman et al[24] described increased hydroxyproline and type α1(I) procollagen associated with the PPE AAA development performed in male Wistar rats, and similarly, we observed increased collagen content in the CAAA wall from 6 to 14 days after PPE exposure. Lysyl oxidases are expressed in the aortic wall, and BAPN inhibits this family of enzymes that catalyze the conversion of lysine residues in collagen and elastin by deamination to allysine. The allysine residue is integral to forming highly stable crosslinks that impart additional mechanical strength to collagen and elastin.[55] In our study, collagen content was determined by trichrome staining and aortic wall fibrotic area percentages were calculated. Considering the same 4 animals that received BAPN and were

harvested 6 days after PPE exposure (BAPN 6d), the collagen content for this group was comparable with that of the CAAA 6d ($P = 0.9$) and RAAA ($P = 0.5$) groups. Furthermore, collagen content for NRAAA 14d animals was somewhat lower than that for CAAA 14d, and the difference approached significance ($P = 0.09$). Comparable values for the CAAA 6d, BAPN 6d, and RAAA groups suggests that there is an initial effect of PPE exposure over the first 6 days, independent of BAPN exposure, which decreases the collagen content of the wall. Therefore, an additional process ensues that causes the fraction of the BAPN-exposed group that ruptures to do so after 6 days post-PPE exposure. The lack of a significant difference in collagen content when comparing CAAA 14d and NRAAA 14d animals suggests that there may have been a deficiency in BAPN administration or a lack of effect with NRAAA 14d animals; alternatively, we propose that NRAAA 14d rats may have been able to remodel the wall and generate enough collagen to help contain the AAA and prevent rupture, whereas RAAA rats did not. Our results support the notion that collagen provides the tensile strength necessary to contain and aneurysmal aorta, and decreased collagen content in the AAA wall increases the risk of AAA rupture.

There are a number of limitations associated with our study. Some of our experimental groups are limited to 3 to 4 rats per group. This is a model of AAA rupture in rats, whereby, we exposed 24 rats to BAPN, with 15 of those rats demonstrating AAA rupture. Although many current AAA basic science studies are performed in mice to take advantage of knockout technologies, most studies using rats utilize only 4 to 8 rats per group.[10,56–58] Another limitation lies in the fact that the PPE model requires significant manipulation of and trauma to the rat aortic wall, and the PPE itself causes an aortitis because of the microbiologic content of the PPE slurry. BAPN has thus far been considered an agent that causes aortic dissection, whereas in our hands, it seems to cause AAA rupture. The requirement for continued administration of BAPN represents a model that again requires persistent mechanical disruption to the aortic wall and not just an inflammatory response from which rupture ensues. In addition, we have not definitively demonstrated that the inflammatory responses that we have visualized with ^{18}F-FDG micro-PET and described at cellular and molecular levels represent processes that cause AAA rupture, as opposed to developing in response to rupture. Given that the process of rupture associated with our model occurs over a matter of minutes, and our limited study of BAPN-exposed animals that were harvested at 6 days post-PPE exposure would suggest that it is an inflammatory response that develops and ultimately stimulates rupture. We will need to study more animals that are exposed to BAPN and are harvested before having the opportunity to rupture. With regard to our imaging studies, we did not coregister our ^{18}F-FDG micro-PET images with higher resolution anatomical imaging, such as computed tomography or magnetic resonance imaging. We did not have access to combined computed tomography/PET at our institution; therefore, this would have required that we perform anatomical imaging in separate, distant locations. Coregistration is possible with the application of mutual information routines; however, we felt that the anesthetic and imaging times would have placed the animals at risk and may have resulted in unnecessary animal loss. Our ability to definitively identify the medial AAA wall is limited by the resolution of micro-PET scanner. However, rupture exclusively occurred in a left anterolateral location, proximal to the aortotomy site, and we were able to resolve the lateral aortic wall without

difficulty. A group of positive control animals were also not imaged at 14 days post-PPE exposure. Four animals experienced rupture 10 days post-PPE exposure; however, given that the negative control group demonstrated decreased ^{18}F-FDG uptake at 14 days, we speculate that the positive control group would have likely demonstrated similarly decreased uptake at 14 days. In the future, we will also need to image more BAPN-exposed animals with ^{18}F-FDG micro-PET, in an effort to better characterize the NRAAA group. The global increase in AAA ^{18}F-FDG uptake seems to represent an increased inflammatory response that we would argue contains the developing AAA, unlike its ruptured counterpart.

CONCLUSIONS

It appears that our use of the BAPN-stimulated PPE model results in infiltration of neutrophils during the acute phase of the model. It may be that the AAA wall that ultimately ruptures does not secrete sufficient levels of PAI-1, and unopposed levels of uPA contributes to macrophage recruitment and MMP9 synthesis as part of the fibrinolytic system utilized for thrombus resolution and AAA wall remodeling. Despite the stimulated remodeling process that seems to be driven in part by IL-6 upregulation, continued inhibition of normally cross-linked collagen deposition by BAPN administration results in a fragile wall that ultimately ruptures (Fig. 4). We have demonstrated the ability to noninvasively assess these inflammatory processes that drive rat AAA rupture utilizing ^{18}F-FDG micro-PET and identify metabolically active sites in a prerupture state that ultimately rupture. Our ability to predict rat AAA rupture suggests that ^{18}F-FDG PET as well as other radiotracers that target increased inflammatory cell presence and/or activity could have a clinical role in predicting AAA rupture in patients.

Supplementary Material

Refer to Web version on PubMed Central for supplementary material.

ACKNOWLEDGMENTS

The authors thank Melissa Bevard, Christopher Strayhorn, Catherine Luke, Megan Elfline, and Dallas Slack for their expertise and assistance with performing histology and immunohistochemistry for this study; Phillip Sherman, Carole Quesada, and Lawrence Holt for their expertise and assistance with performing our micro-PET studies; and Angela Pechota for her expertise and assistance with performing the western blot and zymography experimentation.

The study was supported by the following grants: NIH F32HL103065-01, NIH RO1HL081629-01, and University of Michigan Cardiovascular Center Grant.

REFERENCES

1. Kotze CW, Menezes LJ, Endozo R, et al. Increased metabolic activity in abdominal aortic aneurysm detected by 18F-fluorodeoxyglucose (18F-FDG) positron emission tomography/computed tomography (PET/CT). Eur J Vasc Endovasc Surg. 2009; 38:93–99. [PubMed: 19217326]
2. Sakalihasan N, Van Damme H, Gomez P, et al. Positron emission tomography (PET) evaluation of abdominal aortic aneurysm (AAA). Eur J Vasc Endovasc Surg. 2002; 23:431–436. [PubMed: 12027471]
3. Holmes DR, Petrinec D, Wester W, et al. Indomethacin prevents elastase-induced abdominal aortic aneurysms in the rat. J Surg Res. 1996; 63:305–309. [PubMed: 8661215]

4. Linder AE, Weber DS, Whitesall SE, et al. Altered vascular reactivity in mice made hypertensive by nitric oxide synthase inhibition. J Cardiovasc Pharmacol. 2005; 46:438–444. [PubMed: 16160594]
5. Knipp BS, Ailawadi G, Sullivan VV, et al. Ultrasound measurement of aortic diameters in rodent models of aneurysm disease. J Surg Res. 2003; 112:97–101. [PubMed: 12873440]
6. Knoess C, Siegel S, Smith A, et al. Performance evaluation of the microPET R4 PET scanner for rodents. Eur J Nucl Med Mol Imaging. 2003; 30:737–747. [PubMed: 12536244]
7. Bai B, Li Q, Holdsworth CH, et al. Model-based normalization for iterative 3D PET image reconstruction. Phys Med Biol. 2002; 47:2773–2784. [PubMed: 12200938]
8. Visser EP, Philippens ME, Kienhorst L, et al. Comparison of tumor volumes derived from glucose metabolic rate maps and SUV maps in dynamic 18F-FDG PET. J Nucl Med. 2008; 49:892–898. [PubMed: 18483085]
9. Diaz JA, Booth AJ, Lu G, et al. Critical role for IL-6 in hypertrophy and fibrosis in chronic cardiac allograft rejection. Am J Transplant. 2009; 9:1773–1783. [PubMed: 19538487]
10. Cho BS, Woodrum DT, Roelofs KJ, et al. Differential regulation of aortic growth in male and female rodents is associated with AAA development. J Surg Res. 2009; 155:330–338. [PubMed: 19111327]
11. DiMusto PD, Lu G, Ghosh A, et al. Increased PAI-1 in females compared with males is protective for abdominal aortic aneurysm formation in a rodent model. Am J Physiol Heart Circ Physiol. 2012; 302:H1378–H1386. [PubMed: 22307671]
12. Kotze CW, Groves AM, Menezes LJ, et al. What is the relationship between 18F-FDG aortic aneurysm uptake on PET/CT and future growth rate? Eur J Nucl Med Mol Imaging. 2011; 38:1493–1499. [PubMed: 21468762]
13. Truijers M, Kurvers HA, Bredie SJ, et al. In vivo imaging of abdominal aortic aneurysms: increased FDG uptake suggests inflammation in the aneurysm wall. J Endovasc Ther. 2008; 15:462–467. [PubMed: 18729562]
14. Sakalihasan N, Hustinx R, Limet R. Contribution of PET scanning to the evaluation of abdominal aortic aneurysm. Semin Vasc Surg. 2004; 17:144–153. [PubMed: 15185180]
15. Reeps C, Essler M, Pelisek J, et al. Increased 18F-fluorodeoxyglucose uptake in abdominal aortic aneurysms in positron emission/computed tomography is associated with inflammation, aortic wall instability, and acute symptoms. J Vasc Surg. 2008; 48:417–423. discussion 424. [PubMed: 18572354]
16. Reeps C, Bundschuh RA, Pellisek J, et al. Quantitative assessment of glucose metabolism in the vessel wall of abdominal aortic aneurysms: correlation with histology and role of partial volume correction. Int J Cardiovasc Imaging. 2013; 29:505–512. [PubMed: 22772434]
17. Sarda-Mantel L, Alsac JM, Boisgard R, et al. Comparison of 18F-fluoro-deoxyglucose, 18F-fluoro methyl-choline, and 18F-DPA714 for positron-emission tomography imaging of leukocyte accumulation in the aortic wall of experimental abdominal aneurysms. J Vasc Surg. 2012; 56:765–773. [PubMed: 22726755]
18. Patel R, Janoudi A, Vedre A, et al. Plaque rupture and thrombosis are reduced by lowering cholesterol levels and crystallization with ezetimibe and are correlated with fluorodeoxyglucose positron emission tomography. Arterioscler Thromb Vasc Biol. 2011; 31:2007–2014. [PubMed: 21817102]
19. Darling RC. Ruptured arteriosclerotic abdominal aortic aneurysms: a pathologic and clinical study. Am J Surg. 1970; 119:397–401. [PubMed: 4908753]
20. Assar AN, Zarins CK. Ruptured abdominal aortic aneurysm: a surgical emergency with many clinical presentations. Postgrad Med J. 2009; 85:268–273. [PubMed: 19520879]
21. Killeen S, Neary P, O'Sullivan M, et al. Daily diurnal variation in admissions for ruptured abdominal aortic aneurysms. World J Surg. 2007; 31:1869–1871. [PubMed: 17571206]
22. Kanematsu Y, Kanematsu M, Kurihara C, et al. Pharmacologically induced thoracic and abdominal aortic aneurysms in mice. Hypertension. 2010; 55:1267–1274. [PubMed: 20212272]
23. Rateri DL, Howatt DA, Moorleghen JJ, et al. Prolonged infusion of angiotensin II in ApoE(–/–) mice promotes macrophage recruitment with continued expansion of abdominal aortic aneurysm. Am J Pathol. 2011; 179:1542–1548. [PubMed: 21763672]

24. Huffman MD, Curci JA, Moore G, et al. Functional importance of connective tissue repair during the development of experimental abdominal aortic aneurysms. Surgery. 2000; 128:429–438. [PubMed: 10965315]
25. Lopez-Candales A, Holmes DR, Liao S, et al. Decreased vascular smooth muscle cell density in medial degeneration of human abdominal aortic aneurysms. Am J Pathol. 1997; 150:993–1007. [PubMed: 9060837]
26. Vorp DA, Lee PC, Wang DH, et al. Association of intraluminal thrombus in abdominal aortic aneurysm with local hypoxia and wall weakening. J Vasc Surg. 2001; 34:291–299. [PubMed: 11496282]
27. Hans SS, Jareunpoon O, Balasubramaniam M, et al. Size and location of thrombus in intact and ruptured abdominal aortic aneurysms. J Vasc Surg. 2005; 41:584–588. [PubMed: 15874920]
28. Houard X, Rouzet F, Touat Z, et al. Topology of the fibrinolytic system within the mural thrombus of human abdominal aortic aneurysms. J Pathol. 2007; 212:20–28. [PubMed: 17352452]
29. Heiple JM, Ossowski L. Human neutrophil plasminogen activator is localized in specific granules and is translocated to the cell surface by exocytosis. J Exp Med. 1986; 164:826–840. [PubMed: 3746200]
30. Booth NA, Simpson AJ, Croll A, et al. Plasminogen activator inhibitor (PAI-1) in plasma and platelets. Br J Haematol. 1988; 70:327–333. [PubMed: 3264718]
31. Diaz JA, Ballard-Lipka NE, Farris DM, et al. Impaired fibrinolytic system in ApoE gene-deleted mice with hyperlipidemia augments deep vein thrombosis. J Vasc Surg. 2012; 55:815–822. [PubMed: 22119245]
32. Moore KL, Patel KD, Bruehl RE, et al. P-selectin glycoprotein ligand-1 mediates rolling of human neutrophils on p-selectin. J Cell Biol. 1995; 128:661–671. [PubMed: 7532174]
33. Stewart GJ. Neutrophils and deep venous thrombosis. Haemostasis. 1993; 23(suppl 1):127–140. [PubMed: 8495864]
34. Henke PK, Varga A, De S, et al. Deep vein thrombosis resolution is modulated by monocyte CXCR2 mediated activity in a mouse model. Arterioscler Thromb Vasc Biol. 2004; 24:1130–1137. [PubMed: 15105284]
35. Sho E, Sho M, Nanjo H, et al. Comparison of cell-type-specific vs transmural aortic gene expression in experimental aneurysms. J Vasc Surg. 2005; 41:844–852. [PubMed: 15886670]
36. Capdeville M, Coutard M, Osborne-Pellegrin MJ. Spontaneous rupture of the internal elastic lamina in the rat: the manifestation of a genetically determined factor which may be linked to vascular fragility. Blood Vessels. 1989; 26:197–212. [PubMed: 2575918]
37. Johnston WF, Salmon M, Su G, et al. Genetic and pharmacologic disruption of interleukin-1 beta signaling inhibits experimental aortic aneurysm formation. Arterioscler Thromb Vasc Biol. 2013; 33:294–304. [PubMed: 23288154]
38. Rider P, Carmi Y, Guttman O, et al. IL-1α and IL-1β recruit different myeloid cells and promote different stages of sterile inflammation. J Immunol. 2011; 187:4835–4843. [PubMed: 21930960]
39. Cheuk BL, Cheng SW. Can local secretion of prostaglandin E2, thromboxane B2, and interleukin -6 play a role in ruptured abdominal aortic aneurysm? World J Surg. 2008; 32:55–61. [PubMed: 17992560]
40. Roumen RM, Hendriks T, van der Ven-Jongekrijg J, et al. Cytokine patterns in patients after major vascular surgery, hemorrhagic shock, and severe blunt trauma: relation with subsequent adult respiratory distress syndrome and multiple organ failure. Ann Surg. 1993; 218:769–776. [PubMed: 8257227]
41. Wojcik BM, Wrobleski SK, Hawley AE, et al. Interleukin-6: A potential target for post-thrombotic syndrome. Ann Vasc Surg. 2011; 25:229–239. [PubMed: 21131172]
42. Wallinder J, Skagius E, Bergqvist D, et al. Early inflammatory response in patients with ruptured abdominal aortic aneurysm. Vasc Endovascular Surg. 2010; 44:32–35. [PubMed: 19917558]
43. Lee SR, Guo SZ, Scannevin RH, et al. Induction of matrix metalloproteinase, cytokines and chemokines in rat cortical astrocytes exposed to plasminogen activators. Neurosci Lett. 2007; 417:1–5. [PubMed: 17386975]
44. Gong Y, Hart E, Shchurin A, et al. Inflammatory macrophage migration requires MMP-9 activation by plasminogen in mice. J Clin Invest. 2008; 118:3012–3024. [PubMed: 18677407]

45. Cheuk BL, Cheng SW. Differential secretion of prostaglandin E(2), thromboxane A(2) and interleukin -6 in intact and ruptured abdominal aortic aneurysms. Int J Mol Med. 2007; 20:391–395. [PubMed: 17671746]
46. Hannawa KK, Eliason JL, Woodrum DT, et al. L-selectin-mediated neutrophil recruitment in experimental rodent aneurysm formation. Circulation. 2005; 112:241–247. [PubMed: 15998669]
47. Petersen E, Wagberg F, Angquist KA. Proteolysis of the abdominal aortic aneurysm wall and the association with rupture. Eur J Vasc Endovasc Surg. 2002; 23:153–157. [PubMed: 11863333]
48. Hurks R, Pasterkamp G, Vink A, et al. Circumferential heterogeneity in the abdominal aortic aneurysm wall composition suggests lateral sides to be more rupture prone. J Vasc Surg. 2012; 55:203–209. [PubMed: 21944916]
49. Kurihara T, Shimizu-Hirota R, Shimoda M, et al. Neutrophil-derived matrix metalloproteinase 9 triggers acute aortic dissection. Circulation. 2012; 126:3070–3080. [PubMed: 23136157]
50. Roderfeld M, Graf J, Giese B, et al. Latent MMP-9 is bound to TIMP-1 before secretion. Biol Chem. 2007; 388:1227–1234. [PubMed: 17976016]
51. Khan JA, Abdul Rahman MN, Mazari FA, et al. Intraluminal thrombus has a selective influence on matrix metalloproteinases and their inhibitors (tissue inhibitors of matrix metalloproteinases) in the wall of abdominal aortic aneurysms. Ann Vasc Surg. 2012; 26:322–329. [PubMed: 22305865]
52. Thompson RW, Curci JA, Ennis TL, et al. Pathophysiology of abdominal aortic aneurysms: Insights from the elastase-induced model in mice with different genetic backgrounds. Ann N Y Acad Sci. 2006; 1085:59–73. [PubMed: 17182923]
53. Wilson WR, Anderton M, Choke EC, et al. Elevated plasma MMP1 and MMP9 are associated with abdominal aortic aneurysm rupture. Eur J Vasc Endovasc Surg. 2008; 35:580–584. [PubMed: 18226564]
54. Dobrin PB, Mrkvicka R. Failure of elastin or collagen as possible critical connective tissue alterations underlying aneurysmal dilatation. Cardiovasc Surg. 1994; 2:484–488. [PubMed: 7953454]
55. Remus EW, O'Donnell RE Jr, Rafferty K, et al. The role of lysyl oxidase family members in the stabilization of abdominal aortic aneurysms. Am J Physiol Heart Circ Physiol. 2012; 303:H1067–H1075. [PubMed: 22904155]
56. Cho BS, Roelofs KJ, Ford JW, et al. Decreased collagen and increased matrix metalloproteinase-13 in experimental abdominal aortic aneurysms in males compared with females. Surgery. 2010; 147:258–267. [PubMed: 19767051]
57. Sinha I, Pearce CG, Cho BS, et al. Differential regulation of the superoxide dismutase family in experimental aortic aneurysms and rat aortic explants. J Surg Res. 2007; 138:156–162. [PubMed: 17196988]
58. Sinha I, Cho BS, Roelofs KJ, et al. Female gender attenuates cytokine and chemokine expression and leukocyte recruitment in experimental rodent abdominal aortic aneurysms. Ann N Y Acad Sci. 2006; 1085:367–379. [PubMed: 17182958]

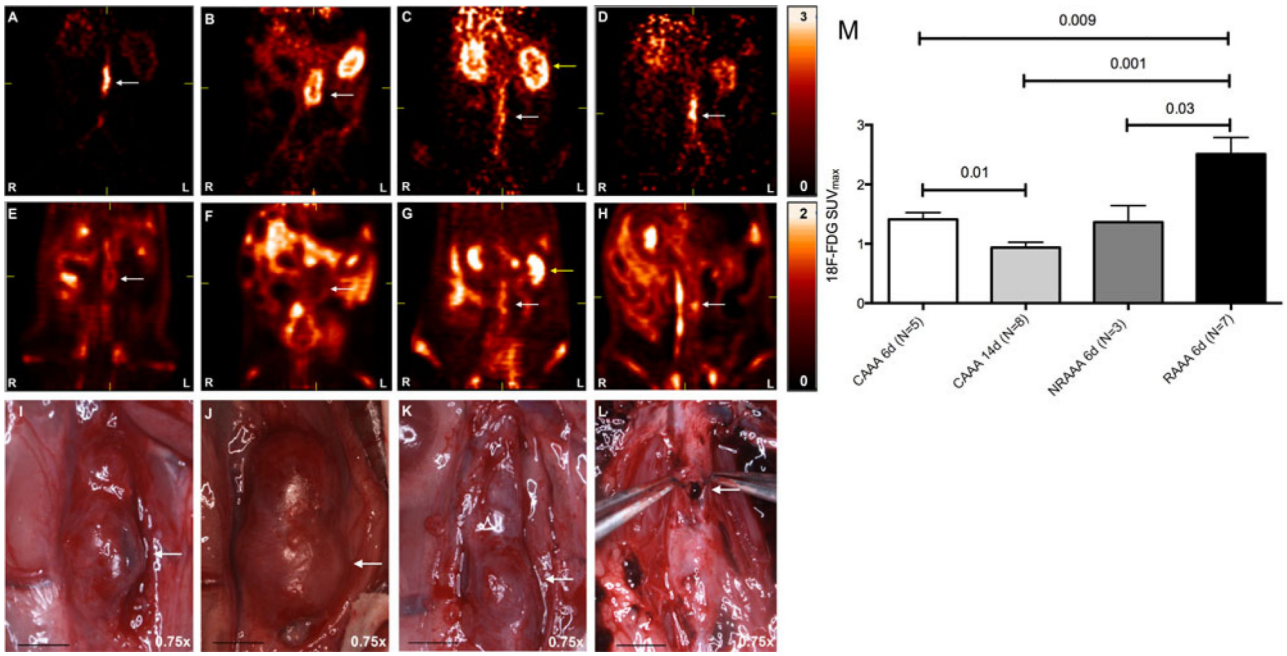

FIGURE 1.

Micro-PET SUV_{max} maps demonstrating increased focal, late phase AAA ^{18}F-FDG uptake at the site of ultimate AAA rupture. Early phase represents the first 90 seconds, and late phase represents the last 30 minutes, of a 90-minute micro-PET scan. (A–D) Coronal cuts for early phase images: (A) CAAA 6d, (B) CAAA 14d, (C) NRAAA 6d, and (D) RAAA 6d. (E–H) Coronal cuts for late phase images: (E) CAAA 6d, (F) CAAA 14d, (G) NRAAA 6d, diffuse AAA ^{18}F-FDG uptake, with decreased uptake in the left anterolateral AAA wall, and (H) RAAA 6d, focal ^{18}F-FDG uptake in the left lateral AAA wall. (I–L) Harvest photographs for the respective animals imaged in A–H, magnification 0.75×, scale bar 5 mm: (I) CAAA 6d, (J) CAAA 14d, (K) NRAAA 6d, and (L) RAAA 6d on harvest, rupture site correlated with the focal ^{18}F-FDG uptake noted in image H. Yellow arrows identify the left kidney. (M) SUV_{max} values for left anterolateral focal ^{18}F-FDG uptake.

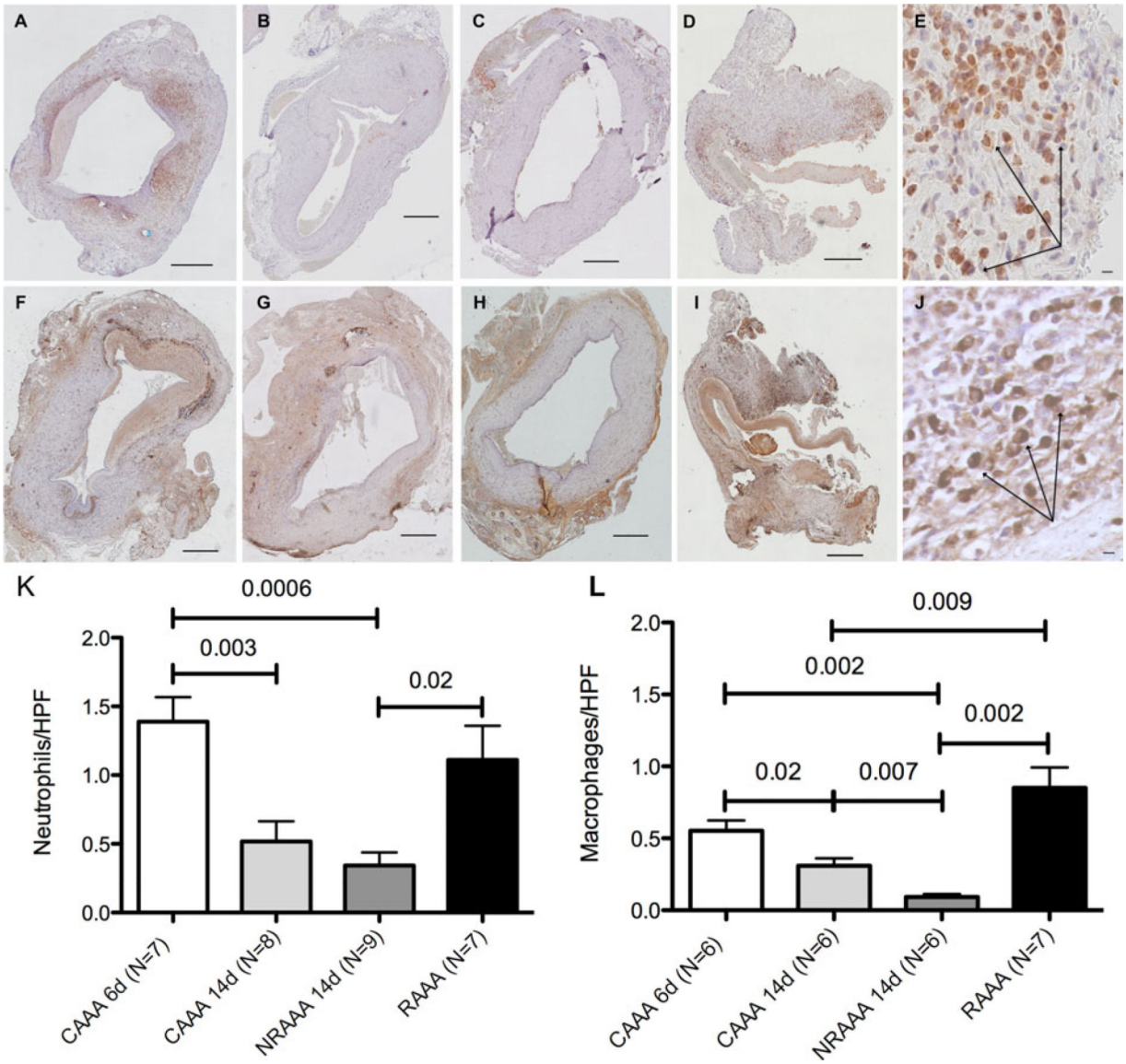

FIGURE 2.

Increased neutrophil and macrophage populations identified utilizing antineutrophil and CD68 immunohistochemistry. Representative antineutrophil stained sections at 10× magnification for (A) CAAA 6d, (B) CAAA 14d, (C) NRAAA 14d, and (D) RAAA sections. (A–D) Scale bar 500 μm. (E) Neutrophils (arrows) adjacent to the site of rupture in the RAAA CD68 stained section at high magnification (63×). Scale bar 10 μm. Representative CD68-stained sections at 10× magnification for (F) CAAA 6d, (G) CAAA 14d, (H) NRAAA 14d, and (I) RAAA sections. (F–I) Scale bar 500 μm. (J) Macrophages (arrows) adjacent to the site of rupture in the RAAA section at high magnification (63×). Scale bar 10 μm. (K) Neutrophil counts per high power field (HPF). (L) Macrophage counts per HPF.

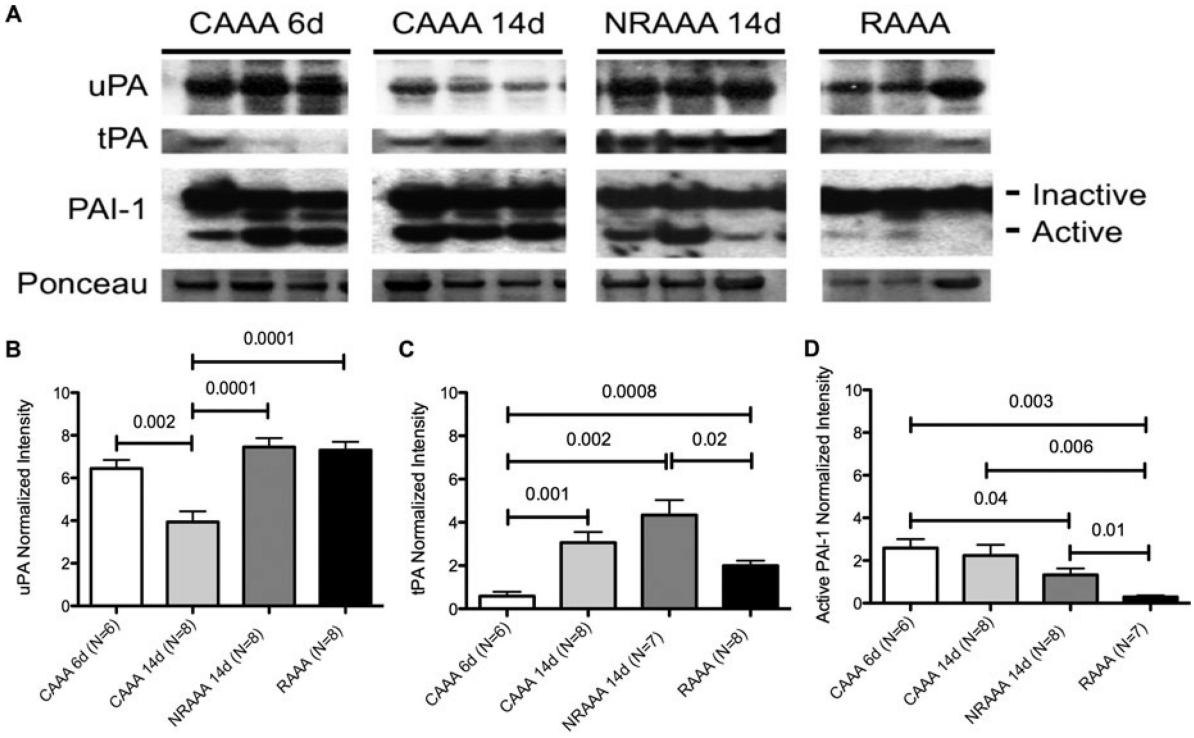

FIGURE 3.

Decreased PAI-1 expression in BAPN-stimulated PPE RAAA tissue. (A) Western blots for uPA, tPA, PAI-1, and Ponceau stain considering CAAA 6d, CAAA 14d, NRAAA 14d, and RAAA tissues. (B) uPA, (C) tPA, and (D) active PAI-1 western blot normalized intensity relative to Ponceau staining. Three representative bands per group were cut from 3 different blots.

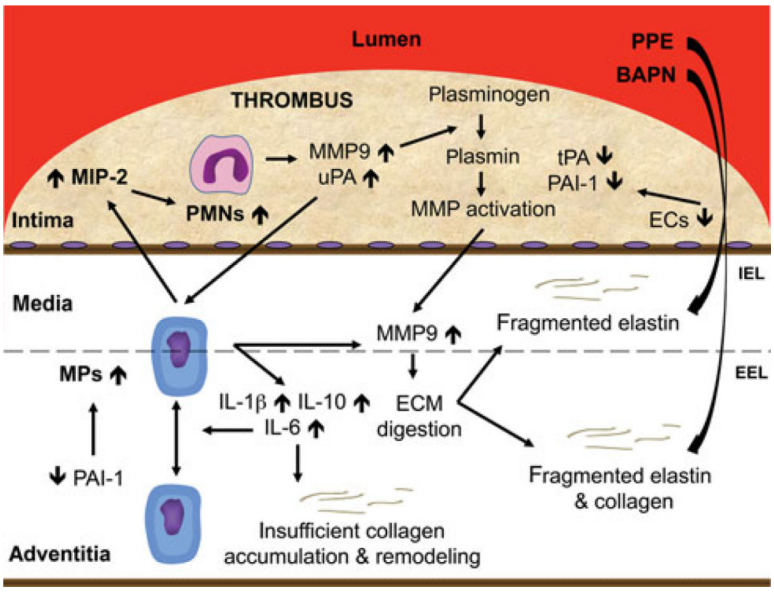

FIGURE 4.

Proposed mechanism for AAA rupture. EEL indicates external elastic lamina; IEL, internal elastic lamina.